

# Cosmological Constraints from 21cm Surveys After Reionization

Eli Visbal,<sup>1,2,\*</sup> Abraham Loeb,<sup>2</sup> and Stuart Wyithe<sup>3</sup>

<sup>1</sup>*Jefferson Laboratory of Physics, Harvard University, Cambridge, MA 02138*

<sup>2</sup>*Harvard-Smithsonian CfA, 60 Garden Street, Cambridge, MA 02138*

<sup>3</sup>*School of Physics, University of Melbourne, Parkville, Victoria, Australia*

(Dated: March 14, 2019)

21cm emission from residual neutral hydrogen after the epoch of reionization can be used to trace the cosmological power spectrum of density fluctuations. Using a Fisher matrix formulation, we provide a detailed forecast of the constraints on cosmological parameters that are achievable with this probe. We consider two designs: a scaled-up version of the MWA observatory as well as a Fast Fourier Transform Telescope. We find that 21cm observations dedicated to post-reionization redshifts may yield significantly better constraints than next generation Cosmic Microwave Background (CMB) experiments. We find the constraints on  $\Omega_\Lambda$ ,  $\Omega_m h^2$ , and  $\Omega_b h^2$  to be the strongest, each improved by at least an order of magnitude over the Planck CMB satellite alone for both designs. In difference from similar 21cm surveys of the epoch of reionization, our results do not depend strongly on uncertainties in the astrophysics associated with the ionization of hydrogen.

## I. INTRODUCTION

Recently, there has been much interest in the feasibility of mapping the three-dimensional distribution of cosmic hydrogen through its spin-flip transition at a resonant rest frame wavelength of 21cm [1, 2]. Several first generation experiments are being constructed to probe the epoch of reionization (MWA [3], LOFAR [4], PAPER [5], 21CMA [6]) and more ambitious designs are being planned (SKA [7]).

One driver for mapping hydrogen through 21cm emission is to measure cosmological parameters from the underlying cosmic power spectrum. During the epoch of reionization (EoR), the 21cm power spectrum is shaped mainly by the structure of ionized regions. Even without precise knowledge of the ionization power spectrum it is possible to isolate the cosmological power spectrum by exploiting anisotropies in redshift space due to peculiar velocities [8, 9].

Recent work [10, 11] has shown that the 21cm power spectrum accessible during the EoR has the potential to put tight constraints on cosmological parameters; however, these constraints depend on model-dependent uncertainties, the most important of which involves the ionization power spectrum.

In this paper, we explore in detail the constraints achievable from mapping the residual cosmic hydrogen after reionization [12, 13, 14, 15, 16, 17]. The hydrogen resides in pockets of dense galactic regions which are self-shielded from the UV background, also known as damped Lyman- $\alpha$  absorbers (DLAs) in quasar spectra [18]. In difference from traditional galaxy redshift surveys, 21cm surveys do not need to resolve individual galaxies but rather are able to monitor the smooth variation in their cumulative 21cm emission owing to their clustering on large scales [15].

Measuring the 21cm power spectrum after reionization offers several key advantages as compared to the EoR. First, the near uniformity of the UV radiation field guarantees that the 21cm power spectrum would reliably trace the underlying matter power spectrum. In addition to making the cosmological signal simpler to extract from observations, this fact eliminates much of the uncertainty in forecasting possible constraints. Another advantage of probing low redshifts is that the brightness temperature of the galactic synchrotron emission scales as  $(1+z)^{2.6}$ . However, this advantage is offset by the fact that the mass weighted neutral fraction of hydrogen is only a few percent at redshifts  $z \lesssim 6$  [19].

In this paper we use the Fisher matrix formalism to quantify how effectively futuristic surveys dedicated to post-reionization redshifts ( $z \lesssim 6$ ) can constrain cosmology. We consider both a survey with ten times the number of cross dipoles of the MWA [3] ( $5000 \times 16 = 8 \times 10^4$ ) but operating at higher frequencies, which we term MWA5000, and a Fast Fourier Transform Telescope (FFTT) with  $10^6$  dipoles over a square kilometer area [20]. We also show results for the combination of these surveys and a next generation Cosmic Microwave Background (CMB) experiment (Planck).

This paper is structured as follows. In §II we discuss the detectability of the 21cm signal after reionization and in §III we discuss its power spectrum. In §IV we consider the details of our Fisher matrix calculation and in §V we present its results for a conservative minimal model and a more detailed astrophysical model. Finally, we discuss and summarize our conclusions in §VI and §VII.

## II. DETECTABILITY OF THE 21CM SIGNAL AFTER REIONIZATION

Reionization starts with ionized (HII) regions around galaxies which grow and eventually overlap. This overlap of HII regions characterizes the end of the EoR. It was once thought that the 21cm signal would disappear after

---

\*[evisbal@fas.harvard.edu](mailto:evisbal@fas.harvard.edu)

this transition because there is little neutral hydrogen left. Recent work has shown that this is not the case [12, 15, 17, 21, 22]. The *detectability* of the signal may not decline substantially following the end of the EoR because the Galactic synchrotron foreground is weaker at higher frequencies (lower redshifts of the 21cm emission).

After reionization most of the remaining neutral hydrogen is expected to reside in DLAs. Observations have shown that out to  $z \approx 4$  the cosmological density parameter of HI is  $\Omega_{\text{HI}} \approx 10^{-3}$  [19]. This corresponds to a mass-averaged neutral fraction of a few percent. It does not contribute significantly to the Ly $\alpha$  forest, which is mostly shaped by the much smaller volume-averaged neutral fraction. A 21cm survey like the ones we discuss are sensitive to all neutral hydrogen within the survey volume because no galaxies are individually identified and thus there is no minimum threshold for the detection of individual galaxies.

Even though the majority of the neutral hydrogen resides in self shielded clumps, self absorption is not expected to significantly reduce the 21cm signal. This is supported by 21cm absorption studies of DLAs over the redshift interval  $0 < z \lesssim 3.4$ , which exhibit an optical depth to 21cm absorption of the radio flux from a background quasar of less than a few percent [23, 24]. These observations are supported by theoretical calculations of the 21cm optical depth of neutral gas in high redshift minihalos [25]. We also note that the spin temperature in DLAs is much higher than the CMB temperature and thus the 21cm signal is independent of the kinetic temperature of the gas [23].

At  $z \approx 4$  the 21cm brightness temperature contrast with the CMB will be roughly 0.5 mK. On scales of 10 comoving Mpc, the *rms* amplitude of density fluctuations is roughly  $\sigma \approx 0.2$ , so we expect 21cm fluctuations at a level of  $\approx 0.1\text{mK}$ . This is only an order of magnitude or so less than the largest fluctuations expected during the EoR [26]. These fluctuations combined with the lower brightness temperature of galactic synchrotron emission, which scales as  $(1+z)^{2.6}$ , should provide a detectable signal. Previous work (e.g. Fig. 10 in Ref.[21]) shows that the signal to noise ratio of the 21cm signal after reionization may be similar or even higher than that during the EoR. However, it is important to note that it will be necessary to build special instruments which are optimized to these redshifts to obtain the type of results discussed in this paper.

### III. 21CM POWER SPECTRUM

Next, we describe the 21cm power spectrum after the epoch of reionization. A complete discussion of the relevant physics can be found in Refs. [1, 12, 15, 17]. The difference between the average brightness temperature of 21cm emission at redshift  $z$  and the CMB temperature

is described by

$$\bar{T}_{\text{b}} \approx 26\bar{x}_{\text{H}} \left( \frac{\bar{T}_{\text{s}} - T_{\text{CMB}}}{\bar{T}_{\text{s}}} \frac{\Omega_{\text{b}} h^2}{0.022} \right) \left( \frac{0.15}{\Omega_{\text{m}} h^2} \frac{1+z}{10} \right)^{1/2} \text{mK}, \quad (1)$$

where  $\bar{x}_{\text{H}}$  is the global neutral hydrogen fraction and  $T_{\text{s}}$  is the HI spin temperature. In Fourier space, the power spectrum of 21cm brightness fluctuations is defined by  $(2\pi)^3 \delta^3(\mathbf{k} - \mathbf{k}') P_{21}(\mathbf{k}) \equiv \langle \Delta T_{\text{b}}(\mathbf{k})^* \Delta T_{\text{b}}(\mathbf{k}') \rangle$ , where  $\mathbf{k}$  is the wave-vector of a given Fourier mode and  $\Delta T_{\text{b}}(\mathbf{k})$  is the brightness temperature fluctuation in Fourier space.

Before giving its exact form, we stress that the most important feature of  $P_{21}(\mathbf{k})$  after reionization is that it essentially traces the cosmological matter power spectrum,  $P(k)$ . Extracting the cosmological power spectrum will make it possible to place tight constraints on many cosmological parameters. During the EoR the situation is more complicated.  $P_{21}(\mathbf{k})$  contains additional terms which depend on the ionization power spectrum and the cross power-spectrum between the ionization and matter distributions.

Following the derivation of Ref. [17] we find that after reionization

$$P_{21}(\mathbf{k}) = \tilde{T}_{\text{b}}^2 \bar{x}_{\text{HI}}^2 P(k) [B(\mathbf{k}) + f\mu^2]^2 \text{mK}. \quad (2)$$

Here  $\tilde{T}_{\text{b}} = \bar{T}_{\text{b}}/(\bar{x}_{\text{HI}}(\bar{T}_{\text{s}} - T_{\text{CMB}})/T_{\text{s}})$ ,  $B(\mathbf{k})$  is the average scale dependent,  $\bar{x}_{\text{HI}}$  mass-weighted bias for the DLA host galaxies, and  $\mu = \cos\theta$  where  $\theta$  is the angle between the line of sight and the wave-vector  $\mathbf{k}$  [17, 22]. The factor  $[B(\mathbf{k}) + f\mu^2]^2$  arises due to redshift space anisotropies from line of sight peculiar velocities [8, 27, 28]. Here the growth index is defined as  $f = d \ln D / d \ln a$ , where  $D(z)$  is the growth factor of density perturbations and  $a$  is the cosmic scale factor. The bias factor arises because the residual neutral hydrogen is located in host galaxies which are biased with respect to the underlying dark matter distribution. This bias and the neutral hydrogen fraction are the only quantities in the above equation which do not depend solely on fundamental physics.

While the near uniformity of the ionizing UV background causes  $P_{21}(\mathbf{k})$  to trace the cosmological power spectrum, fluctuations introduce a modulation that is non-degenerate with cosmological parameters. This modulation of the power spectrum adds a scale dependent correction factor to the host galaxy bias [17]. The average bias  $B(\mathbf{k})$  is equal to the mean halo bias  $b$ , multiplied by a factor  $(1 + K(k))$  with

$$K(k) = K_{\text{o}} \left( 1 + \frac{k}{k_{\text{mfp}}} \right)^{-1}, \quad (3)$$

where  $k_{\text{mfp}}$  is the wavenumber corresponding to the mean-free-path of ionizing photons,  $\lambda_{\text{mfp}} = 85((1+z)/4)^{-4} \text{Mpc}$  [29]. This correction factor arises because on scales much larger than  $\lambda_{\text{mfp}}$  we expect the ionizing background to follow the galaxy density field. This has the effect of suppressing power. On scales

smaller than  $\lambda_{\text{mfp}}$  we expect the ionizing background to be much closer to the mean value diminishing the suppression of power relative to larger scales. We find that incorporating this effect into the Fisher matrix calculation has a very small effect on the results.

The bias,  $b$ , for halos of a particular mass  $M$  can be derived using the Press-Schechter formalism modified to include non-spherical collapse [30]

$$b(M, z) = 1 + \frac{1}{\delta_c} \left[ \nu'^2 + b\nu'^{2(1-c)} - \frac{\nu'^{2c}/\sqrt{a}}{\nu'^{2c} + b(1-c)(1-c/2)} \right], \quad (4)$$

where  $\nu'^2 = a\delta_c^2/\sigma^2(M, z)$ ,  $a = 0.707$ ,  $b = 0.5$ , and  $c = 0.6$ . Here  $\sigma^2(M, z)$  is the variance of the density field smoothed on a mass scale  $M$  and  $\delta_c$  is the linear overdensity threshold for collapse at redshift  $z$ .

Assuming that the neutral gas to halo mass ratio is independent of mass, we can derive the mean bias at a particular redshift,  $\bar{b}$ , as the weighted average

$$\bar{b} = \frac{\int_{M_{\text{min}}}^{\infty} \frac{dn}{dM} b(M, z) M dM}{\int_{M_{\text{min}}}^{\infty} \frac{dn}{dM} M dM}, \quad (5)$$

where  $dn/dM$  is the Sheth-Tormen mass function of dark matter halos [30]. The minimum halo mass  $M_{\text{min}}$  defines the threshold for assembling heated gas out of the photo-ionized intergalactic medium, corresponding to a minimum virial temperature  $T_{\text{vir}} \approx 10^5 K$  [31, 32, 33, 34, 35, 36]. A constant virial temperature leads to the redshift dependence  $M_{\text{min}} = 5.3 \times 10^9 ((1+z)/4.5)^{-1.5} M_{\odot}$ . Based on observations of DLAs [19], we parametrize the neutral hydrogen density to linear order,  $x_{\text{HI}} = x_{\text{HI1}} + x_{\text{HI2}}(z - z_{\text{center}})$ , with the fiducial choices of  $x_{\text{HI1}} = 0.02$  and  $x_{\text{HI2}} = 0$ .

### A. Non-Linear Effects on Baryon Acoustic Oscillations

It has been recently shown that non-linear effects may change the baryon acoustic oscillations (BAO) signature at much larger scales than previously thought [37]. The erasure of BAO information due to non-linear effects can be written as

$$P_{\text{b, nl}}(k, \mu) = P_{\text{b, lin}}(k, \mu) \times \exp \left[ -\frac{k^2}{2} \left( (1 - \mu^2) \Sigma_{\perp}^2 + \mu^2 \Sigma_{\parallel}^2 \right) \right], \quad (6)$$

where  $P_{\text{b}}$  is the part of the power spectrum which contains the wiggles from the BAO,  $\Sigma_{\perp} = \Sigma_0 \tilde{D}(z)$ ,  $\Sigma_{\parallel} = \Sigma_0(1+f)\tilde{D}(z)$ ,  $\Sigma_0 = 11.6h^{-1}\text{Mpc}$ , and  $\tilde{D}(z)$  is the growth function normalized to  $(1+z)^{-1}$  at high redshifts. Our choice of  $\Sigma_0$  corresponds to the value determined by simulations and scaled linearly with  $\sigma_8$  to fit our fiducial cosmology. In all of our Fisher matrix calculations we marginalize over  $\Sigma_0$ .

## IV. FISHER MATRIX FORMULATION

Given a set of parameters  $\lambda_i$ , the Fisher matrix formalism provides an estimation of the error for each of the parameters associated with some data set [38]. The  $1\sigma$  errors on parameters can be estimated as

$$\Delta\lambda_i = \sqrt{F_{ii}^{-1}}, \quad (7)$$

where

$$F_{ij} = \sum_{\text{pixels}} \frac{1}{\delta P_{12}^2} \left( \frac{\partial P_{21}}{\partial \lambda_i} \right) \left( \frac{\partial P_{21}}{\partial \lambda_j} \right), \quad (8)$$

[9, 10],  $P_{21}$  is the total 21cm power spectrum, and  $\delta P_{21}$  is the uncertainty on a measurement of the power spectrum. The relevant derivatives have been calculated using the transfer functions from CAMB [39].

We work in  $\mathbf{u}$ -space rather than  $\mathbf{k}$ -space as described in Refs. [9, 10] to simplify calculating Alcock-Paczynski effects. A radio interferometer directly measures visibilities,

$$V(u, v, \nu) = \int d\hat{\mathbf{n}} \Delta T_{\text{b}}(\hat{\mathbf{n}}, \nu) A_{\nu}(\hat{\mathbf{n}}) e^{2\pi i(u, v) \cdot \hat{\mathbf{n}}}, \quad (9)$$

where  $V$  is the visibility for a pair of antennae and  $A_{\nu}$  is the contribution to the primary beam in the  $\hat{\mathbf{n}}$  direction. Here we have used the flat sky approximation. This is appropriate even in the case of the FFTT, which images the entire hemisphere, because essentially all of the cosmological information in our surveys is found on small angular scales. The vector  $\mathbf{u}_{\perp} = (u, v)$  corresponds to the number of wavelengths between the pair of antennae. Performing the Fourier transform  $I(\mathbf{u}) = \int d\nu V(u, v, \nu) \exp(2\pi i\nu\eta)$ , we obtain a signal in terms of  $\mathbf{u} = u\hat{\mathbf{i}} + v\hat{\mathbf{j}} + \eta\hat{\mathbf{k}}$ , where  $\eta$  has units of time and  $\hat{\mathbf{k}}$  is the unit vector along the line of sight. Note that there is a one to one correspondence between  $\mathbf{k}$  and  $\mathbf{u}$  given by  $2\pi\mathbf{u}_{\perp}/d_A = \mathbf{k}_{\perp}$  perpendicular to the line of sight and  $2\pi\mathbf{u}_{\parallel}/\tilde{y} = \mathbf{k}_{\parallel}$  along the line of sight, where  $d_A$  is the angular diameter distance to the observation and  $\tilde{y}$  is the ratio of comoving distance to frequency interval. With the Fourier conventions above we have  $P_{21}(\mathbf{k}) = P_{21}(\mathbf{u})d_A^2\tilde{y}$ . Working in  $\mathbf{u}$ -space simplifies our calculation because  $P_{21}(\mathbf{u})$  is measurable without cosmological assumptions and thus Eq. (8) can be applied directly. If we were to work in  $\mathbf{k}$ -space, the Alcock-Paczynski effect would distort  $P_{21}(\mathbf{k})$  from Eq. (2) when we take derivatives with respect to cosmological parameters.

Because we are considering discrete sources, the total 21cm power spectrum will be the sum of Eq. (2) and a shot noise term  $P_{\text{shot}} = P_{21}(k)/(b^2 P(k)n_{\text{DLA}})$ , where  $n_{\text{DLA}}$  is the number density of the galaxies which host DLAs,  $P_{21}(k)$  is  $P_{21}(\mathbf{k})$  along the line of sight, and  $b^2 P(k)$  is the power spectrum of DLA hosting galaxies along the line of sight.

Any constant  $|\mathbf{k}|$  and  $\theta$  define an annulus of constant  $P_{21}(\mathbf{u})$ . The Fisher matrix is calculated from Eq. (8) by

summing the contribution from annuli which fill all of  $\mathbf{k}$ -space accessible to an observation. We divide a 21cm survey into redshift bins small enough for the redshift evolution of  $P(k)$  across a bin to be negligible. A separate Fisher matrix is calculated for each redshift bin and then summed into a Fisher matrix which reflects the information about the entire survey.

To calculate the error in Eq. (8) we follow the work of Refs. [9, 40]. The error on  $P_{21}$  for a particular  $|\mathbf{k}|$  and  $\theta$  is

$$\delta P_{21} = \frac{P_{21} + P_{\text{shot}} + P_N}{\sqrt{N_c \times N_{\text{fields}} \times B_{\text{tot}}/B}}, \quad (10)$$

where  $P_N$  is the noise power spectrum of an interferometer,  $B$  is the bandwidth over which foregrounds can be removed,  $B_{\text{tot}}$  is the total accessible bandwidth,  $N_{\text{fields}}$  is the number of fields being imaged, and  $N_c$  is the number of independent cells in  $\mathbf{k}$ -space. The number of cells in an annulus of constant  $P_{21}(\mathbf{u})$  is well approximated by

$$N_c = 2\pi k^2 \sin \theta \Delta k \Delta \theta \frac{V}{(2\pi)^2}, \quad (11)$$

where  $V$  is the comoving volume observed by the experiment,  $\Delta \theta$  and  $\Delta k$  are the angular and  $\mathbf{k}$ -space widths of the annulus. We choose  $\Delta k$  and  $\Delta \theta$  such that  $P_{21}(\mathbf{u})$  is essentially constant. The noise of an interferometer is given by

$$P_N(u_\perp) = \left( \frac{\lambda^2 T_{\text{sys}}}{A_e} \right)^2 \frac{1}{t_0 n(u_\perp)}, \quad (12)$$

where  $\lambda = 21\text{cm} \times (1+z)$  is the observed wavelength,  $T_{\text{sys}}$  is the system temperature of the interferometer,  $A_e$  is the effective area,  $t_0$  is the total observing time, and  $n(u_\perp)$  is the number density of baselines. This error is identical to that applicable in studies of the EoR with the exception of the shot noise [9, 10].

The sensitivity of 21cm measurements will be impacted by how effectively foregrounds such as the galactic synchrotron emission can be removed. Refs. [9, 41, 42] suggest that after fitting out a low order polynomial, residual foregrounds in the power spectrum will be negligible if the frequency band over which foregrounds are removed,  $B$ , is substantially smaller than the total band-pass available. This is true for wave-vectors greater than  $k_{\text{min}} = 2\pi/(\hat{y}B)$ . Recent work estimating errors on cosmological parameters with 21cm surveys during the EoR has used this assumption in modeling foreground removal [9, 10, 11]. It is encouraging that we find parameter constraints to depend relatively weakly on the exact value of the bandwidth over which foregrounds are removed (see Fig. 2). We note that while we expect these assumptions pertaining to foreground removal to be robust, the true ability to remove foregrounds may not be known until first generation 21cm instruments are operational.

There are several factors which limit the scales accessible to 21cm surveys for parameter determination. As

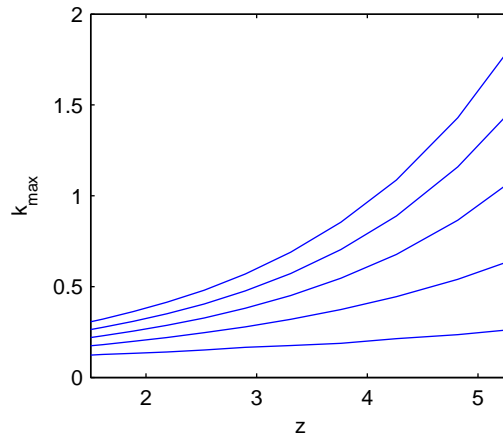


FIG. 1: Maximal wavenumber,  $k_{\text{max}}$ , above which the non-linear power-spectrum deviates from the linear power-spectrum by more than 25%, 20%, 15%, 10% and 5% (top to bottom). Larger discrepancies produce higher values of  $k_{\text{max}}$ .

discussed above, we assume that foregrounds can not be effectively removed from pixels with  $k < k_{\text{min}}$ . There is also a minimum accessible value of  $k \sin \theta$  imposed by the minimum baseline,  $b_{\text{min}} \approx \sqrt{A_{\text{phys}}}$ . We exclude information for  $k$  values above the linear scale. We compare the linear power spectrum for our fiducial cosmology to a non-linear power spectrum produced by HALOFIT in CAMB [39], and define our non-linear cutoff as the  $k$  value where there is a 10% discrepancy. The value of this cutoff is fairly conservative when compared to the criterion of Ref. [43] which chooses  $k_{\text{nl}} = \pi/2R$  for a value of  $R$  giving an *rms* density fluctuation amplitude  $\sigma(R) = 0.5$ . The latter criterion has been used for 21cm parameter constraints at higher redshifts than we explore [11]. We find that the parameter constraints are not very sensitive to increasing the discrepancy that determines  $k_{\text{max}}$ . The  $k_{\text{max}}$  values corresponding to different levels of discrepancy between the linear and non-linear power spectra are shown in Fig. 1. The effects of changing  $k_{\text{max}}$  on cosmological constraints will be discussed later (see Fig. 3).

We also include constraints when combined with future data from the Planck satellite [44]. The method used to calculate the corresponding Fisher matrix was adopted from Refs. [45, 46].

### A. Survey Characteristics

We apply the Fisher matrix formulation to future surveys dedicated to low redshifts similar in design to MWA5000 and a Fast Fourier Transform Telescope (FFTT). We show results with surveys designed for a central redshift of 3.5 and 1.5 that each span a factor of 3 in  $(1+z)$ .

We model the MWA5000 observatory as an interferom-

eter with 5000 tiles each containing 16 dipole antennae. For the survey centered at  $z = 3.5(1.5)$  we assume a constant core of antennae out to 40(22)m and then a  $r^{-2}$  distribution out to 500(278)m. This layout gives roughly the same baseline density distribution as MWA does at higher redshifts [9].

For the survey centered around  $z = 3.5$  the effective area of each tile  $A_e \approx N_{\text{dip}}\lambda^2/4$  and is limited by the physical area of the tile,  $A_{\text{phys}}$  [47]. The values of  $A_{\text{phys}}$  are chosen such that  $A_{\text{phys}} \approx A_e$  at the central redshift. For the low-redshift case, we assume that dishes are used instead of antennae, resulting in  $A_e \approx A_{\text{phys}}$ .

We model an FFTT observatory [20] as an interferometer with  $10^6$  evenly spaced dipoles over a square kilometer that can all be correlated. The noise in each dipole is calculated separately with  $A_e \approx \lambda^2/4$  limited by  $A_{\text{phys}} = S^2$ , where  $S$  is the spacing of the dipoles on a square grid.

We have assumed that foregrounds can be removed on scales of up to  $30[4.5/(1+z)]\text{MHz}$ . This corresponds to the value that [15] cite as desirable to measure the neutrino signal. The exact choice of this bandwidth is relatively unimportant, as our results depend weakly on this value (see Fig. 2). We assume that 0.65 of the sky in one hemisphere is imaged for 2000 hours. This corresponds to roughly 16 fields of view. The partial coverage is due to foregrounds which can not be removed in the vicinity of the galactic plane. We also show results for a more conservative case using MWA5000 over three fields of view rather than 16.

For all surveys we assume a redshift range corresponding to a factor of 3 in frequency and break each observation into redshift bins of width  $\Delta z = 0.1(1+z)$ . The factor of 3 corresponds to the largest frequency bandwidth over which a low frequency dipole antenna has suitable sensitivity. In our lower redshift case we have assumed that dishes will be used. These could potentially have a larger bandwidth than the dipole antennae, but we conservatively use the same factor of 3 in frequency. We also assume that  $T_{\text{sys}} = T_{\text{sky}} + T_{\text{inst}}$  where the sky temperature  $T_{\text{sky}} = 260[(1+z)/9.5]^{2.55}$  [48], and that the instrumental temperature is 30K in an optimistic case and 100K in a pessimistic case, corresponding to what is reasonable with current technology and what might be expected by the time the hypothetical experiments we discuss will be built.

## B. Cosmological Parameters

Throughout this work we assume that the true background cosmology is that of a flat  $\Lambda\text{CDM}$  Universe with density parameters  $\Omega_\Lambda = 0.7$  in dark energy,  $\Omega_m h^2 = 0.147$  in matter,  $\Omega_b h^2 = 0.023$  in baryons, and  $\Omega_\nu h^2 = 0.00054$  in neutrinos, and with values of  $A_s^2 = 25.0 \times 10^{-10}$ ,  $n_s = 0.95$ , and  $\alpha = 0.0$  for the spectral index, amplitude, and running of the primordial power spectrum. The chosen value of  $A_s$  corresponds to

an  $rms$  fluctuation amplitude on a  $8h^{-1}$  Mpc scale of  $\sigma_8 = 0.84$ . We have assumed a neutrino hierarchy with one dominant species having a neutrino mass of 0.05eV. We assume a fiducial value of  $\tau = 0.1$  for the optical depth to electron scattering during reionization, and a helium mass fraction from big bang nucleosynthesis of  $Y_{\text{He}} = 0.24$ . In a lower redshift example we also leave the dark energy equation of state as a free parameter with a fiducial value of  $w = -1$ .

## V. RESULTS

We present the results of our Fisher matrix calculations in Tables I-VI. To illustrate the robustness of our constraints we compare both a simple model that expresses almost all of the relevant astrophysics in terms of free parameters and a more detailed astrophysical model which makes specific assumptions. In both cases we show constraints for both optimistic and pessimistic antenna temperature. We also show results for a cosmic variance limited version of each survey where the detector noise is assumed to make no contribution. This case represents the best conditions imaginable for constraining cosmological parameters given the finite volume of space that is observed. As it turns out, an FFTT is essentially cosmic variance limited at the redshifts of interest here. In this case, we only show results for the optimistic antenna temperature case.

As previously stated, we assume a flat  $\Lambda\text{CDM}$  cosmology except for one case centered around  $z = 1.5$  where we leave  $w$  as a free parameter.

### A. Minimal Model

We begin with a conservative minimal model where we have made essentially no assumptions about the background astrophysics. In this model, we assume that both the shot noise as well as the bias in each redshift bin are unknown. Each is marginalized over as a free parameter in the Fisher matrix. We use Eqs. (4) and (5) to determine the fiducial values of these parameters in each bin. The results are presented in Tables I-IV.

### B. Astrophysical Model

Next we present results for calculations with a more ambitious astrophysical model. Here we assume that there is one DLA per dark matter halo above a threshold mass for assembling heated gas from the intergalactic medium,  $M_{\text{min}}$ , which we parametrize as  $M_{\text{min}} = M_0(1+z/4.5)^\beta$ . In the fiducial case we have set  $\beta = -1.5$  and  $M_0 = 5.3 \times 10^9 M_\odot$ . This corresponds to a constant virial temperature. The value of  $M_{\text{min}}$  is used to set the bias and the galaxy density in each redshift bin. Both  $M_0$  and  $\beta$  are left as parameters

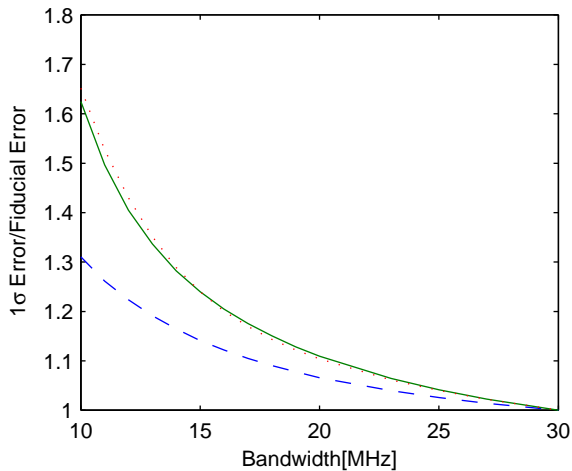


FIG. 2: Sensitivity of the relative  $1\sigma$  error bar to the bandwidth over which foregrounds can be removed for FFTT. Errors have been normalized such that they equal unity for the assumptions in Table I. The dashed line gives the error for  $\Omega_\Lambda$ , the dotted line for  $\Omega_\nu h^2$ , and the solid line for  $n_s$ .

that must be measured and thus are marginalized over in our Fisher matrix calculation. We also include the scale dependent modulation of the bias due the ionization field implied by Eq. (2). We parametrize the mean free path as  $\lambda_{\text{mfp}} = A_{\text{mfp}} \left(\frac{1+z}{4}\right)^{B_{\text{mfp}}}$  with fiducial values of  $A_{\text{mfp}} = 85\text{Mpc}$  and  $B_{\text{mfp}} = -4.0$ . We marginalize over  $A_{\text{mfp}}$ ,  $B_{\text{mfp}}$ , and  $K_0$  (see Eq. (3)). We have chosen  $K_0 = -0.5$  for the fiducial case. Marginalizing over ionization parameters has a small effect on the results. In general, we find that degeneracies associated with the ionization parameters increase the  $1\sigma$  errors on cosmological parameters by less than 20% for 21cm surveys and Planck combined. In many cases the parameter errors are essentially unchanged.

Our constraints are presented in Tables V and VI. Because we find these results to be very similar to the minimal model, we only include a table for only one case, MWA5000 viewing 65% of one hemisphere centered around  $z = 3.5$ .

### C. Other Factors

There are several other factors that affect the constraints attainable with post-reionization 21cm surveys. We investigate how these factors change our constraints in the minimal model. In Fig. 2, we have plotted the dependence of the  $1\sigma$  uncertainty on the bandwidth over which foregrounds are removed. Larger values for the bandwidth allow measurement of smaller  $k$  values which are otherwise not accessible. Overall, the sensitivity to the bandwidth variation is relatively modest.

In Fig. 3, we show how the constraints vary for different choices of  $k_{\text{max}}$ , the maximum wavenumber being

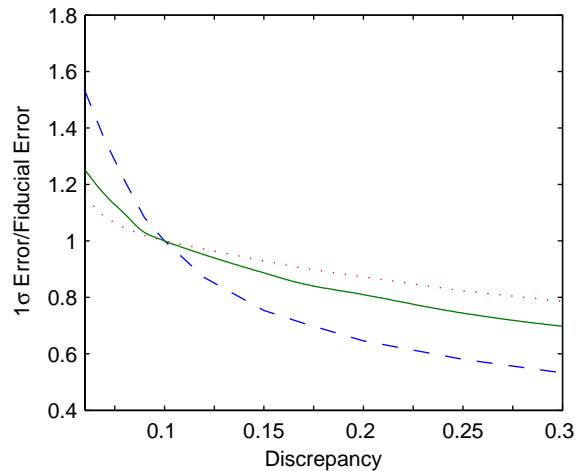


FIG. 3: Sensitivity of the relative  $1\sigma$  error bar to the maximal wavenumber  $k_{\text{max}}$  for FFTT. Errors have been normalized such that they equal one for the assumptions in Table I. The dashed line gives the error for  $\Omega_\Lambda$ , the dotted line for  $\Omega_\nu h^2$ , and the solid line for  $n_s$ .

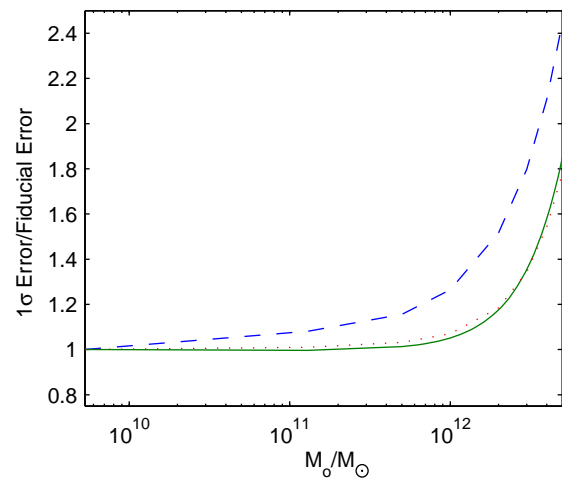


FIG. 4: Dependence of constraints on  $M_0$  for FFTT. Errors have been normalized such that they equal one for the assumptions in table I. The dashed line gives the error for  $\Omega_\Lambda$ , the dotted line for  $\Omega_\nu h^2$ , and the solid line for  $n_s$ .

used. We show how the parameter uncertainties change if we impose the cutoff at different levels of discrepancy between the non-linear and linear power spectra. Again, the resulting variations appear to be relatively small.

In Fig. 4, we show how the constraints depend on  $M_{\text{min}}$ , the minimum halo mass above which significant amounts of neutral hydrogen may assemble. A high value of  $M_{\text{min}}$  increases the shot noise and degrades the constraints. We find that the shot noise only affects the results significantly above  $\sim 10^{12} M_\odot$ , which is unrealistic since hydrogen is found in lower mass galaxies in the

local Universe [49].

## VI. DISCUSSION

Our constraints on cosmological parameters are similar in the minimal and detailed astrophysical model, implying a weak dependence on the astrophysics or other factors (see Figs. 2-4). For comparison, the constraints from 21cm surveys that focus on the EoR [10] vary by two orders of magnitude under different model assumptions. The robustness of our post-reionization constraints is mainly due to the fact that we do not have to consider the ionization power spectrum.

The noise in the interferometers is lower at lower redshift due to the redshift scaling of the galactic synchrotron emission. This advantage is offset by the fact that at higher redshifts the neutral fraction is higher and the observed power spectrum stays linear up to a higher  $k_{\text{max}}$  value. While the FFTT is essentially cosmic variance limited, the MWA5000 with the optimistic antenna temperature has errors that are about twice as large at  $z = 3.5$  and almost the same at  $z = 1.5$ . These experiments would be close to capturing all the information available from the power spectrum available to us on linear scales at the relevant redshifts.

Current cosmological information sets the upper limit on neutrino mass to  $\sim 0.62$  eV [50, 51]. For FFTT we find a  $1\sigma$  error corresponding to 0.038eV. As expected [15], this is clearly much better than existing constraints and is sufficiently small to probe the neutrino mass differences implied by neutrino oscillations.

It is also interesting to compare how well these surveys constrain cosmology with respect to other future probes. The FFTT and the MWA5000 survey over a hemisphere will both perform much better than the Planck satellite for almost all of the parameters under consideration. When combined with Planck, essentially all of the constraints are improved. In Table IV we explicitly show how the constraint on each parameter from Planck would improve if combined with post-reionization 21cm surveys. The most improved parameters are  $\Omega_{\Lambda}$ ,  $\Omega_{\text{m}}h^2$ , and  $\Omega_{\nu}h^2$ ,

which for FFTT are 3.3%, 5.1%, and 8.4% of the errors from Planck alone.

In the case where we allow  $w$  to vary as a free parameter we find the constraints on most parameters essentially unchanged. The main exception is  $\Omega_{\Lambda}$ , where we find that our constraints are increased by roughly a factor of two. The constraints achievable for  $w$  are interesting, about 5% if the whole hemisphere is observed, and 10% with only three fields of view.

## VII. CONCLUSIONS

A 21cm survey after reionization provides a promising probe of cosmology and fundamental physics [15]. We find that our forecasted constraints do not depend strongly on the details of astrophysics modeling in difference from EoR surveys where assumptions about the ionization power spectrum introduce model-dependent uncertainties into the final constraints [10, 11].

Aside from its greater simplicity, the measurement sensitivity after reionization is improved over EoR surveys due to lower foreground brightness temperature, a bias that is greater than unity, and a larger growth factor of density perturbations. These advantages are somewhat offset by the fact that there is less neutral hydrogen after reionization.

The constraints we derive are competitive with those from the EoR and significantly better than next generation CMB experiments on their own. We find errors on  $\Omega_{\Lambda}$ ,  $\Omega_{\text{m}}h^2$ , and  $\Omega_{\nu}h^2$  to be improved the most, each lowering the errors from Planck alone by at least an order of magnitude for both FFTT and the survey similar in design to MWA5000.

## Acknowledgments

This work was supported in part by a NASA LA grant and by Harvard University funds. We thank Matt McQuinn and Jonathan Pritchard for useful discussions.

- 
- [1] S. Furlanetto, S. P. Oh, and F. Briggs, *Phys. Rept.* **433**, 181 (2006).
  - [2] R. Barkana and A. Loeb, *Reports on Progress in Physics* **70**, 627 (2007).
  - [3] <http://www.haystack.mit.edu/ast/arrays/mwa>.
  - [4] <http://www.lofar.org>.
  - [5] <http://www.astro.berkeley.edu/dbacker/EoR>.
  - [6] <http://web.phys.cmu.edu/past>.
  - [7] <http://www.skatelescope.org>.
  - [8] R. Barkana and A. Loeb, *Astrophys. J.* **624**, L65 (2005).
  - [9] M. McQuinn, O. Zahn, M. Zaldarriaga, L. Hernquist, and S. R. Furlanetto, *Astrophys. J.* **653**, 815 (2006).
  - [10] Y. Mao, M. Tegmark, M. McQuinn, M. Zaldarriaga, and O. Zahn, *Phys. Rev. D* **78**, 023529 (2008).
  - [11] J. R. Pritchard and E. Pierpaoli, *Phys. Rev. D* **78**, 065009 (2008).
  - [12] S. Wyithe and A. Loeb, *Mon. Not. Roy. Astron. Soc.* **383**, 606 (2007).
  - [13] J. S. B. Wyithe, A. Loeb, and P. M. Geil, *Mon. Not. Roy. Astron. Soc.* **383**, 1195 (2008).
  - [14] T.-C. Chang, U.-L. Pen, J. B. Peterson, and P. McDonald, *Phys. Rev. Lett.* **100**, 091303 (2008).
  - [15] A. Loeb and J. S. B. Wyithe, *Physical Review Letters* **100**, 161301 (2008).
  - [16] U.-L. Pen, L. Staveley-Smith, J. Peterson, and T.-C. Chang, *ArXiv e-prints* (2008), 0802.3239.

TABLE I: Min model:  $1\sigma$  Errors on cosmological parameters with surveys centered at  $z = 3.5$ . OPT refers to an antenna temperature of 30K, PESS 100K, and CVL to the cosmic variance limited case. OPT and PESS correspond to what may be possible by the time these experiments will be built and what is achievable today.

Fiducial Values		$\Omega_\Lambda$	$\Omega_m h^2$	$\Omega_b h^2$	$n_s$	$A_s^2 \times 10^{10}$	$\alpha$	$\Omega_\nu h^2$	$\tau$	$Y_{\text{He}}$	$x_{\text{HI1}}$	$x_{\text{HI2}}$
MWA5k-Hemisphere		PESS	0.0026	0.0019	0.00048	0.0068	–	0.0039	0.00064	–	0.00058	0.000087
		OPT	0.002	0.00097	0.00025	0.0051	–	0.003	0.00052	–	0.00037	0.00007
		CVL	0.0012	0.00025	0.000083	0.0035	–	0.0014	0.0004	–	0.00018	0.000046
MWA5k-3 Fields		PESS	0.0061	0.0043	0.0011	0.016	–	0.0092	0.0015	–	0.0014	0.0002
		OPT	0.0048	0.0023	0.00058	0.012	–	0.0069	0.0012	–	0.00087	0.00016
		CVL	0.0027	0.00058	0.00019	0.0082	–	0.0034	0.00093	–	0.00042	0.00011
FFTT			0.0013	0.00027	0.000086	0.0036	–	0.0016	0.00041	–	0.0002	0.000049
Planck			0.038	0.0041	0.00024	0.0094	0.25	0.007	0.0039	0.0046	0.014	–
+MWA5k-Hemisphere			0.002	0.00038	0.00012	0.0032	0.21	0.002	0.0004	0.004	0.005	0.0003
+MWA5k-3 Fields			0.0046	0.00063	0.00016	0.0047	0.22	0.0028	0.00073	0.0041	0.0065	0.00063
+FFTT			0.0013	0.00021	0.000077	0.0029	0.2	0.0013	0.00034	0.004	0.0044	0.0002

<sup>a</sup>When not otherwise indicated the “OPT” value of  $T_{\text{sys}}$  has been used.

<sup>b</sup>For cases without Planck,  $x_{\text{HI1}}$  and  $x_{\text{HI2}}$  errors are actually errors of the products of these with  $A_s^2$ .

TABLE II: Min model:  $1\sigma$  Errors on cosmological parameters with surveys centered at  $z = 1.5$ . OPT refers to an antenna temperature of 30K, PESS 100K, and CVL to the cosmic variance limited case. OPT and PESS correspond to what may be possible by the time these experiments will be built and what is achievable today.

Fiducial Values		$\Omega_\Lambda$	$\Omega_m h^2$	$\Omega_b h^2$	$n_s$	$A_s^2 \times 10^{10}$	$\alpha$	$\Omega_\nu h^2$	$\tau$	$Y_{\text{He}}$	$x_{\text{HI1}}$	$x_{\text{HI2}}$
MWA5k-Hemisphere		PESS	0.0032	0.015	0.0038	0.032	–	0.01	0.0019	–	0.0036	0.00013
		OPT	0.0028	0.011	0.0029	0.025	–	0.0083	0.0016	–	0.0027	0.00011
		CVL	0.0026	0.0099	0.0026	0.022	–	0.0077	0.0014	–	0.0024	0.000099
MWA5k-3 Fields		PESS	0.0075	0.035	0.009	0.074	–	0.024	0.0045	–	0.0084	0.0003
		OPT	0.0064	0.026	0.0067	0.058	–	0.019	0.0037	–	0.0064	0.00025
		CVL	0.006	0.023	0.006	0.052	–	0.018	0.0034	–	0.0057	0.00023
Planck			0.038	0.0041	0.00024	0.0094	0.25	0.0070	0.0039	0.0046	0.014	–
+MWA5k-Hemisphere			0.0022	0.00041	0.00015	0.0044	0.22	0.0035	0.00053	0.0041	0.0066	0.00026
+MWA5k-3 Fields			0.0049	0.00066	0.00019	0.0066	0.22	0.0048	0.00091	0.0041	0.0096	0.00046

<sup>a</sup>When not otherwise indicated the “OPT” value of  $T_{\text{sys}}$  has been used.

<sup>b</sup>For cases without Planck,  $x_{\text{HI1}}$  and  $x_{\text{HI2}}$  errors are actually errors of the products of these with  $A_s^2$ .

- [17] S. Wyithe and A. Loeb, ArXiv e-prints (2008), 0808.2323.
- [18] A. M. Wolfe, E. Gawiser, and J. X. Prochaska, *Ann. Rev. Astron. Astrophys.* **43**, 861 (2005).
- [19] J. X. Prochaska, S. Herbert-Fort, and A. M. Wolfe, *Astron. Astrophys. J.* **635**, 123 (2005).
- [20] M. Tegmark and M. Zaldarriaga, ArXiv e-prints **805** (2008), 0805.4414.
- [21] J. R. Pritchard and A. Loeb, *Phys. Rev.* **D78**, 103511 (2008).
- [22] S. Wyithe, *Mon. Not. Roy. Astron. Soc.* **388**, 1889 (2008).
- [23] N. Kanekar and J. N. Chengalur, *Astron. Astrophys.* **399**, 857 (2003).
- [24] S. J. Curran, P. Tzanavaris, M. T. Murphy, J. K. Webb, and Y. M. Pihlstrom, *Mon. Not. Roy. Astron. Soc.* **381**, L6 (2007).
- [25] S. Furlanetto and A. Loeb, *Astron. Astrophys. J.* **579**, 1 (2002).
- [26] S. Wyithe and M. Morales, *Mon. Not. Roy. Astron. Soc.* **379**, 1647 (2007).
- [27] N. Kaiser, *Mon. Not. Roy. Astron. Soc.* **227**, 1 (1987).
- [28] S. Bharadwaj and S. S. Ali, *Mon. Not. Roy. Astron. Soc.* **352**, 142 (2004).
- [29] C. A. Faucher-Giguere, A. Lidz, L. Hernquist, and M. Zaldarriaga, *Astron. Astrophys. J.* **688**, 85 (2008).
- [30] R. K. Sheth, H. J. Mo, and G. Tormen, *Mon. Not. Roy. Astron. Soc.* **323**, 1 (2001).
- [31] S. Wyithe and A. Loeb, *Nature* **441**, 332 (2006).
- [32] G. Efstathiou, *Mon. Not. Roy. Astron. Soc.* **256**, 43P (1992).
- [33] P. R. Shapiro, M. L. Giroux, and A. Babul, *Astron. Astrophys. J.* **427**, 25 (1994).
- [34] A. A. Thoul and D. H. Weinberg, *Astron. Astrophys. J.* **465**, 608 (1996).
- [35] L. Hui and N. Y. Gnedin, *Mon. Not. Roy. Astron. Soc.* **292**, 27 (1997).
- [36] A. Mesinger and M. Dijkstra, *Mon. Not. Roy. Astron. Soc.* **390**, 1071 (2008).
- [37] H.-J. Seo and D. J. Eisenstein, *Astron. Astrophys. J.* **665**, 14 (2007).
- [38] M. Tegmark, A. N. Taylor, and A. F. Heavens, *Astron. Astrophys. J.* **480**, 22 (1997).
- [39] <http://camb.info/>.
- [40] M. F. Morales, *Astron. Astrophys. J.* **619**, 678 (2005).
- [41] X.-M. Wang, M. Tegmark, M. Santos, and L. Knox, *Astron. Astrophys. J.* **650**, 529 (2006).
- [42] V. Jelić, S. Zaroubi, P. Labropoulos, R. M. Thomas, G. Bernardi, M. A. Brentjens, A. G. de Bruyn, B. Ciardi, G. Harker, L. V. E. Koopmans, et al., *Mon. Not. Roy. Astron. Soc.* **389**, 1319 (2008).
- [43] H.-J. Seo and D. J. Eisenstein, *Astron. Astrophys. J.* **598**, 720 (2003).
- [44] <http://sci.esa.int/planck/>.
- [45] G. Jungman, M. Kamionkowski, A. Kosowsky, and D. N. Spergel, *Phys. Rev. D* **54**, 1332 (1996).
- [46] M. Zaldarriaga and U. Seljak, *Phys. Rev. D* **55**, 1830 (1997).
- [47] J. D. Bowman, M. F. Morales, and J. N. Hewitt, *Astron. Astrophys. J.* **638**, 20 (2006).
- [48] A. E. E. Rogers and J. D. Bowman (2008), 0806.2868.

TABLE III: Min model:  $1\sigma$  Errors on cosmological parameters with surveys centered at  $z = 1.5$  with  $w$  as a free parameter. OPT refers to an antenna temperature of 30K, PESS 100K, and CVL to the cosmic variance limited case. OPT and PESS correspond to what may be possible by the time these experiments will be built and what is achievable today.

		$\Omega_\Lambda$	$\Omega_m h^2$	$\Omega_b h^2$	$n_s$	$A_s^2 \times 10^{10}$	$\alpha$	$\Omega_\nu h^2$	$w$	$\tau$	$Y_{He}$	$x_{HI1}$	$x_{HI2}$
Fiducial Values		0.7	0.147	0.023	0.95	25.0	0.0	0.00054	-1	0.10	0.24	0.02	0.0
MWA5k-Hemisphere	PESS	0.0057	0.015	0.0038	0.032	–	0.011	0.0024	0.045	–	–	0.0036	0.00039
	OPT	0.0054	0.011	0.0029	0.025	–	0.0088	0.002	0.042	–	–	0.0027	0.00035
	CVL	0.0053	0.01	0.0026	0.023	–	0.0081	0.0019	0.041	–	–	0.0024	0.00033
MWA5k-3 Fields	PESS	0.013	0.035	0.009	0.075	–	0.025	0.0056	0.11	–	–	0.0084	0.00092
	OPT	0.013	0.026	0.0068	0.058	–	0.02	0.0047	0.098	–	–	0.0064	0.00081
	CVL	0.012	0.023	0.006	0.053	–	0.019	0.0044	0.096	–	–	0.0057	0.00077
Planck		0.096	0.0061	0.00024	0.0094	0.27	0.0071	0.0059	0.16	0.0051	0.015	–	–
+MWA5k-Hemisphere		0.0044	0.00047	0.00016	0.0045	0.22	0.0035	0.00059	0.023	0.0041	0.0066	0.00029	0.00017
+MWA5k-3 Fields		0.0095	0.00083	0.00019	0.0066	0.22	0.0048	0.001	0.045	0.0041	0.0096	0.00056	0.00035

<sup>a</sup>When not otherwise indicated the “OPT” value of  $T_{sys}$  has been used.

<sup>b</sup>For cases without Planck,  $x_{HI1}$  and  $x_{HI2}$  errors are actually errors of the products of these with  $A_s^2$ .

TABLE IV: Ratio of  $1\sigma$  Errors for surveys combined with Planck to Errors from Planck alone.

		$\Omega_\Lambda$	$\Omega_m h^2$	$\Omega_b h^2$	$n_s$	$A_s^2$	$\alpha$	$\Omega_\nu h^2$	$\tau$	$Y_{He}$
MWA5k-Hemisphere	$z = 3.5$	0.053	0.091	0.5	0.34	0.83	0.28	0.1	0.86	0.34
MWA5k-3 Fields	$z = 3.5$	0.12	0.15	0.68	0.5	0.87	0.41	0.19	0.88	0.45
FFT	$z = 3.5$	0.033	0.051	0.32	0.31	0.81	0.18	0.085	0.85	0.3
MWA5k-Hemisphere	$z = 1.5$	0.057	0.099	0.64	0.47	0.87	0.5	0.13	0.88	0.45
MWA5k-3 Fields	$z = 1.5$	0.13	0.16	0.79	0.7	0.9	0.68	0.23	0.89	0.66

<sup>a</sup>The “OPT” value of  $T_{sys}$  (30K) and the conservative minimal model have been used.

[49] J. I. Davies et al., Mon. Not. Roy. Astron. Soc. **328**, 1151 (2001).

[50] A. Goobar, S. Hannestad, E. Mortsell, and H. Tu, JCAP **0606**, 019 (2006).

[51] U. Seljak, A. Slosar, and P. McDonald, JCAP **0610**, 014 (2006).

TABLE V: Astrophysical Model:  $1\sigma$  errors on cosmological parameters with surveys centered at  $z = 3.5$ . OPT refers to an antenna temperature of 30K, PESS 100K, and CVL to the cosmic variance limited case. OPT and PESS correspond to what may be possible by the time these experiments will be built and what is achievable today.

Fiducial Values		$\Omega_\Lambda$	$\Omega_m h^2$	$\Omega_b h^2$	$n_s$	$A_s^2 \times 10^{10}$	$\alpha$	$\Omega_\nu h^2$
		0.7	0.147	0.023	0.95	25.0	0.0	0.00054
MWA5k-Hemisphere	PESS	0.0024	0.0019	0.00048	0.0076	–	0.0032	0.00065
	OPT	0.0018	0.00093	0.00024	0.0052	–	0.0021	0.00051
	CVL	0.00088	0.00023	0.000079	0.0032	–	0.001	0.00038

TABLE VI: Astrophysical Model:  $1\sigma$  errors for model parameters with surveys centered at  $z = 3.5$ . OPT refers to an antenna temperature of 30K, PESS 100K, and CVL to the cosmic variance limited case. OPT and PESS correspond to what may be possible by the time these experiments will be built and what is achievable today.

Fiducial Values		$M_O [10^9 M_\odot]$	$\beta$	$K_O$	$A_{\text{mfp}} [Mpc]$	$B_{\text{mfp}}$
		5.3	-1.5	-0.5	85	-4.0
MWA5k-Hemisphere	PESS	11	0.13	0.0067	2.5	0.058
	OPT	7.6	0.096	0.0053	2.1	0.044
	CVL	4.3	0.057	0.0036	1.6	0.028